Mutational Analysis of the *Shigella flexneri* O-Antigen Polymerase Wzy: Identification of Wzz-Dependent Wzy Mutants

Pratiti Nath, Elizabeth Ngoc Hoa Tran, Renato Morona

Discipline of Microbiology and Immunology, School of Molecular and Biomedical Science, University of Adelaide, Adelaide, Australia

The O-antigen (Oag) component of lipopolysaccharide (LPS) is a major virulence determinant of *Shigella flexneri* and is synthesized by the O-antigen polymerase, Wzy_{Sf}. Oag chain length is regulated by chromosomally encoded Wzz_{Sf} and pHS-2 plasmid-encoded Wzz_{pHS2}. To identify functionally important amino acid residues in Wzy_{Sf}, random mutagenesis was performed on the *wzy*$_{Sf}$ gene in a pWaldo-TEV-GFP plasmid, followed by screening with colicin E2. Analysis of the LPS conferred by mutated Wzy_{Sf} proteins in the *wzy*$_{Sf}$-deficient (Δwzy) strain identified 4 different mutant classes, with mutations found in periplasmic loop 1 (PL1), PL2, PL3, and PL6, transmembrane region 2 (TM2), TM4, TM5, TM7, TM8, and TM9, and cytoplasmic loop 1 (CL1) and CL5. The association of Wzy_{Sf} and Wzz_{Sf} was investigated by transforming these mutated *wzy*$_{Sf}$ plasmids into a *wzy*$_{Sf}$- and *wzz*$_{Sf}$-deficient ($\Delta wzy \Delta wzz$) strain. Comparison of the LPS profiles in the Δwzy and $\Delta wzy \Delta wzz$ backgrounds identified Wzy_{Sf} mutants whose polymerization activities were Wzz_{Sf} dependent. Colicin E2 and bacteriophage Sf6c sensitivities were consistent with the LPS profiles. Analysis of the expression levels of the Wzy_{Sf}-GFP mutants in the Δwzy and $\Delta wzy \Delta wzz$ backgrounds identified a role for Wzz_{Sf} in Wzy_{Sf} stability. Hence, in addition to its role in regulating Oag modal chain length, Wzz_{Sf} also affects Wzy_{Sf} activity and stability.

*S*higella flexneri lipopolysaccharide (LPS) is crucial for pathogenesis [1]. LPS is located exclusively in the outer leaflet of the outer membrane (OM) and has three domains: (i) lipid A, a hydrophobic domain that anchors LPS to the OM; (ii) the core oligosaccharides, a nonrepeating oligosaccharide domain; and (iii) the O-antigen (Oag) polysaccharide, an oligosaccharide repeat domain [1, 2]. The complete LPS structure with Oag chains is termed smooth LPS (S-LPS). However, the LPS structure lacking the Oag is termed rough LPS (R-LPS), and LPS with a single Oag tetrasaccharide repeat unit (RU) attached to the lipid A and core sugar is termed semirough LPS (SR-LPS) [3]. *S. flexneri* is subdivided into various serotypes depending on the differences in the composition of the LPS Oag. So far, there are 17 known serotypes of *S. flexneri* [4]. Except for *S. flexneri* serotype 6, the Oags of all the serotypes have the same polysaccharide backbone containing three L-rhamnose residues (Rha) and one *N*-acetylglucosamine (GlcNAc). This basic Oag structure is known as serotype Y. Addition of either glucosyl, *O*-acetyl, or phosphoethanolamine (PEtN) groups by various linkages to the sugars of the Y serotype tetrasaccharide repeat creates different *S. flexneri* serotypes [5–7]. Oag is the protective antigen, as immunity to *S. flexneri* infection is serotype specific [8, 9]. S-LPS confers resistance to complement [10] and colicins [11, 12], and Y serotype Oag acts as a receptor to bacteriophage Sf6 [13].

S. flexneri Oag biosynthesis occurs by the Wzy-dependent pathway. Most of the Oag biosynthesis genes (except *wecA*) of *S. flexneri* are located in the Oag biosynthesis locus between *galF* and *his* [6, 14]. *S. flexneri* Oag biosynthesis occurs on either side of the inner membrane (IM). Initially, *N*-acetylglucosamine phosphate (GlcNAc-1-P) is transferred from UDP-GlcNAc by WecA to undecaprenol phosphate (Und-P) at the cytoplasmic side of the IM [5, 15, 16]. RfbG and RfbF then add Rha residues from dTDP-rhamnose (dTDP-Rha) to the GlcNAc [3, 17] to form the O unit. In the Wzy-dependent model of LPS assembly, the flippase protein Wzx translocates this O unit to the periplasmic side. At the periplasmic side, the O units are polymerized at the nonreducing

end by the Oag polymerization protein Wzy via a block transfer mechanism to form the polymer. The chain length of the final Oag is regulated by the protein Wzz [3, 18]. Finally, the Oag ligase WaaL ligates the Oag chains to the previously synthesized core-lipid A. The Lpt proteins (LptA to -G) then transport the LPS from the IM to the OM [1, 19].

The *S. flexneri* Oag polymerization protein Wzy_{Sf} is encoded by the *rfc* or *wzy* gene. Wzy_{Sf} is a 43.7-kDa hydrophobic integral membrane protein. It has 12 transmembrane (TM) segments and two large periplasmic-loop (PL) domains [3, 18]. Based on a topology model proposed by our group, the amino- and carboxy-terminal ends are located on the cytoplasmic side of the IM. The wild-type *wzy*$_{Sf}$ gene lacks a detectable ribosome binding site and has a low G+C%, and a high percentage of minor codons in the first 25 amino acids, contributing to low expression and poor detection of the protein [3, 18].

Islam et al. [20] performed extensive work on *Pseudomonas aeruginosa* Wzy (Wzy_{Pa}) and showed that both PL3 and PL5 of Wzy_{Pa} contain $RX_{10}G$ motifs, which are important for the functioning of Wzy_{Pa}. They also found that several Arg residues within these two motifs are also important for Wzy_{Pa} function [20]. However, there is little sequence identity between Wzy_{Pa} and

Wzy$_{Sf}$, so it is not possible to predict the functional amino acid residues of Wzy$_{Sf}$ from another model.

Wzz is a member of the polysaccharide copolymerase (PCP) family. *S. flexneri* has two types of Wzz, chromosomally encoded Wzz$_{Sf}$ and pHS-2 plasmid-encoded Wzz$_{pHS2}$. *S. flexneri* 2a has S-LPS with two types of modal chain length: short (S) type (11 to 17 Oag RUs) and very long (VL) type (>90 Oag RUs), and the S-type and VL-type Oag chain lengths are determined by Wzz$_{Sf}$ and Wzz$_{pHS2}$, respectively. Controlling Oag chain length is crucial for bacterial virulence, and loss of Wzz$_{Sf}$-mediated Oag modal chain length regulation affects virulence due to masking of the OM protein IcsA (21, 22). Daniels and Morona showed that Wzz$_{Sf}$ forms a dimer *in vivo* and may oligomerize up to a hexamer (23). Formation of these large complexes is consistent with the hypothetical complex formation between Wzz and other enzymes of the Oag biosynthesis pathway, including Wzy (14, 24). Wzz$_{Sf}$ and Wzz$_{pHS2}$ compete for the available Wzy$_{Sf}$ (25).

Woodward et al. showed that Wzz and Wzy are sufficient to determine the Oag modal chain length (26). There are several proposed mechanisms for modal length control by Wzz and its association with Wzy: a molecular-clock model was proposed by Bastin et al. (24), and a molecular-chaperone model was proposed by Morona et al. (14). Tocilj et al. suggested that Wzz may form a scaffold and that it recruits Wzy (27). However, there is no direct evidence to date on how these proteins are associated with each other in Oag polymerization and chain length control.

In this study, we were able to overexpress and detect Wzy$_{Sf}$-green fluorescent protein (GFP) expression in *S. flexneri*. We performed random mutagenesis on *wzy*$_{Sf}$, and following screening with colicin E2, for the first time identified amino acid residues important for Wzy$_{Sf}$ function. We classified the *wzy*$_{Sf}$ mutants based on their LPS profiles. We were able to determine mutant protein expression levels and also characterized the mutants depending on the phage and colicin sensitivities they conferred. These findings provided insight into Wzy structure and function. We further identified Wzz$_{Sf}$-dependent Wzy$_{Sf}$ mutants and identified a novel role for Wzz$_{Sf}$ in Wzy$_{Sf}$ Oag polymerization activity and stability, in addition to its role in regulating Oag modal chain length.

MATERIALS AND METHODS

Bacterial strains and plasmids. The strains and plasmids used in this study are shown in Table 1.

Growth media and growth conditions. The growth media used were Luria-Bertani (LB) broth (10 g/liter tryptone, 5 g/liter yeast extract, 5 g/liter NaCl) and LB agar (LB broth, 15 g/liter Bacto agar).

Unless otherwise stated, strains were grown in LB broth with aeration for 18 h at 37°C and then diluted 1/20 into fresh LB broth and grown to mid-exponential phase (optical density at 600 nm [OD$_{600}$], 0.4 to 0.6). Where required, the growth medium was supplemented with 0.2% (wt/vol) glucose to suppress protein expression. Before induction, cells were centrifuged (2,200 × *g*; Sigma 3K15 tabletop centrifuge; 10 min; 4°C) and washed twice with LB broth to remove glucose. Under induction conditions, 0.4 mM isopropyl-β-D-thiogalactopyranoside (IPTG) or 0.2% (wt/vol) L-arabinose was added to the cultures, and they were grown for 20 h at 20°C. Antibiotics were added as required to the media at the following final concentrations: kanamycin (Km), 50 μg/ml, and chloramphenicol (Cm), 25 μg/ml.

Construction of expression vector and cloning of *wzy*$_{Sf}$. Primers PN1_*wzy*$_{Sf}$KpnF and PN2_*wzy*$_{Sf}$BamHR (see Table S1 in the supplemental material), which incorporated KpnI and BamHI restriction sites, respectively, were used to amplify the previously mutated *wzy*$_{Sf}$ coding re-

gion (GenBank accession number X71970) in the pRMCD6 plasmid (Table 1), possessing three changes at codons 4, 9, and 23 (18). The rare codons 4, 9, and 23 are present in the translation initiation site of Wzy$_{Sf}$ and cause lower expression of the wild-type Wzy$_{Sf}$. The codons ATA, ATA, and AGA at 4, 9, and 23 were changed to ATT, ATT, and CGT, respectively, and resulted in increased expression of Wzy$_{Sf}$ (18). Following restriction digestion with enzymes BamHI and KpnI, the amplified *wzy*$_{Sf}$ was ligated into similarly digested pWaldo-TEV-GFP (28), resulting in the plasmid pWaldo-*wzy*$_{Sf}$-TEV-GFP (denoted pRMPN1). PCR, restriction enzyme digestion, agarose gel electrophoresis, ligation, and transformation were performed as described previously (3, 14).

Wzy$_{Sf}$ expression in Lemo21(DE3) and in-gel fluorescence. For Wzy$_{Sf}$ expression in Lemo21(DE3) cells (Table 1), strains were induced with IPTG, and the overexpressed Wzy$_{Sf}$-GFP fusion protein was detected by in-gel fluorescence following the method of Drew et al. (29) with some modifications. Cells (5 × 10^8) were harvested from the induced culture and washed twice in 200 μl phosphate buffered-saline (PBS). The pellet was resuspended in 20 μl PBS, and 20 μl buffer A (200 mM Tris-HCl [pH 8.8], 20% [vol/vol] glycerol, 5 mM EDTA [pH 8.0], 0.02% [wt/vol] bromophenol blue, 4% [wt/vol] SDS, and 0.05 M dithiothreitol [DTT]) was then added to the cell suspension. The solubilized cell suspension was incubated at 37°C for 5 min. Samples were then separated by SDS-polyacrylamide gel electrophoresis (PAGE) on 15% (wt/vol) gels, and a BenchMark Pre-Stained Protein Ladder (Invitrogen) was used as a molecular mass standard. The gel was rinsed with distilled water, and fluorescence imaging of the gel was performed to detect Wzy$_{Sf}$-GFP protein expression with a Bio-Rad Gel Doc XR+ system using Image Lab software (excitation at 485 nm and emission at 512 nm).

LPS method. LPS was prepared as described previously (30, 31). To prepare LPS samples, 1 × 10^9 cells were harvested, resuspended in lysing buffer (buffer B, 10% [wt/vol] glycerol, 2% [wt/vol] SDS, 4% [wt/vol] β-mercaptoethanol, 0.1% [wt/vol] bromophenol blue, 1 M Tris-HCl, pH 7.6), and incubated with 2 μg/ml of proteinase K for approximately 16 h. The LPS samples were then electrophoresed on SDS–15% PAGE gels for 16 to 18 h at 12 mA. Gels were stained with silver nitrate and developed with formaldehyde (30).

Random mutagenesis. Random mutagenesis of *wzy*$_{Sf}$ was undertaken to obtain a wide range of *wzy*$_{Sf}$ mutations in a nonselected manner. For PCR random mutagenesis, the *wzy*$_{Sf}$ coding region in plasmid pRMPN1 was mutagenized with an error-prone DNA polymerase using the GeneMorph II EZ-Clone Domain Mutagenesis Kit (catalog number 200552; Stratagene) according to the manufacturer's instructions with the primers PN1_*wzy*$_{Sf}$KpnF and PN2_*wzy*$_{Sf}$BamHR (see Table S1 in the supplemental material). The mutagenized plasmids were transformed into competent *Escherichia coli* XL10-Gold (XL10G) cells (Agilent Technologies). Plasmid DNA was then isolated from randomly chosen transformed, mutated colonies and transformed into strain PNRM6 (Table 1). Colicin swab assays were performed to screen the mutants (see below). Plasmid DNA was isolated from putative mutants, transformed into XL10G cells, and subjected to DNA sequencing (AGRF, Adelaide, Australia).

Construction of the strain RMA4437 (Δ*wzy* Δ*wzz*). The *S. flexneri* Y PE638 Δ*wzy* Δ*wzz* mutant strain was constructed using allelic-exchange mutagenesis (14) to inactivate the *wzz*$_{Sf}$ gene in RMM109 (3). Initially, a tetracycline resistance (Tet^r) cartridge was inserted into the BglII site of pRMA577 (14) to inactivate *wzz*$_{Sf}$, and the resulting pCACTUS-*wzz*$_{Sf}$::*tet* (Table 1) plasmid was transformed into RMM109 via electroporation (32). Allelic-exchange mutagenesis was performed as previously described (14). The *wzz*$_{Sf}$::Tet^r mutation in the chromosome was confirmed by PCR with primers ET35 and ET36 (see Table S1 in the supplemental material) to give the PE638 Δ*wzy* Δ*wzz* mutant RMA4337.

Detection of Wzy$_{Sf}$ expression in *S. flexneri*. For the detection of Wzy$_{Sf}$ expression in *S. flexneri*, cells were harvested from the 50-ml 0.2% (wt/vol) L-arabinose-induced culture by centrifugation (9,800 × *g*; Beckman J2-21M induction drive centrifuge; 10 min; 4°C), and the cell pellet was resuspended in 4 ml sonication buffer (buffer C, 20 mM Tris-HCl,

TABLE 1 Bacterial strains and plasmids used in this study

Strain or plasmid	Characteristics[a]	Reference or source
Strains		
S. flexneri		
PE638	*S. flexneri* Y *rpoB* (Rif^r)	14
RMM109	PE638 Δ*wzy*; Rif^r	3
RMA4337	RMM109 Δ*wzz* (Rif^r Tet^r)	This study
PNRM6	RMM109(pAC/pBADT7-1)	This study
PNRM11	PNRM6(pWaldo-TEV-GFP)	This study
PNRM13	PNRM6(pRMPN1)	This study
PNRM75	PNRM6(pRMPN7)	This study
PNRM76	PNRM6(pRMPN8)	This study
PNRM77	PNRM6(pRMPN9)	This study
PNRM78	PNRM6(pRMPN10)	This study
PNRM79	PNRM6(pRMPN11)	This study
PNRM80	PNRM6(pRMPN12)	This study
PNRM81	PNRM6(pRMPN13)	This study
PNRM82	PNRM6(pRMPN14)	This study
PNRM83	PNRM6(pRMPN15)	This study
PNRM84	PNRM6(pRMPN16)	This study
PNRM85	PNRM6(pRMPN17)	This study
PNRM119	PNRM6(pRMPN19)	This study
PNRM120	PNRM6(pRMPN21)	This study
PNRM121	PNRM6(pRMPN22)	This study
PNRM122	PNRM6(pRMPN23)	This study
PNRM123	PNRM6(pRMPN24)	This study
PNRM124	PNRM6(pRMPN25)	This study
PNRM126	RMA4337(pAC/pBADT7-1)	This study
PNRM134	PNRM126(pRMPN1)	This study
PNRM131	PNRM126(pRMPN7)	This study
PNRM132	PNRM126(pRMPN15)	This study
PNRM133	PNRM126(pRMPN16)	This study
PNRM136	PNRM126(pRMPN8)	This study
PNRM137	PNRM126(pRMPN10)	This study
PNRM140	PNRM126(pRMPN13)	This study
PNRM141	PNRM126(pRMPN14)	This study
PNRM142	PNRM126(pRMPN9)	This study
PNRM143	PNRM126(pRMPN11)	This study
PNRM144	PNRM126(pRMPN19)	This study
PNRM145	PNRM126(pRMPN24)	This study
PNRM146	PNRM126(pRMPN25)	This study
PNRM147	PNRM126(pRMPN23)	This study
PNRM148	PNRM126(pRMPN21)	This study
PNRM149	PNRM126(pRMPN22)	This study
PNRM150	PNRM126(pRMPN12)	This study
PNRM151	PNRM126(pRMPN17)	This study
E. coli		
XL10G	Tet^r Δ(*mcrA*)183 Δ(*mcrCB-hsdSMR-mrr*)173 *endA1 supE44 thi-1 recA1 gyrA96 relA1 lac* [F′ *proAB lacI^{q}Z*ΔM15 Tn*10* (Tet^r) Cm^r]	Stratagene
Lemo21(DE3)	*fhuA2* (*lon*) *ompT gal* (λ DE3) (*dcm*) Δ*hsdS*/pLemo (Cm^r)	New England Biolabs
PNRM15	Lemo21(DE3)(pRMPN1)	This study
Plasmids		
pRMCD6	Source of *wzy$_{Sf}$* (modified codons at positions 4, 9, and 23)	18
pAC/pBADT7-1	Source of T7 RNA polymerase; Cm^r	34
pWaldo-TEV-GFP	Cloning vector with GFP tag; Km^r	28
pRMPN1	pWaldo-*wzy$_{Sf}$*-GFP; Km^r	This study
pRMPN7	pRMPN1 with G130V point mutation in the *wzy$_{Sf}$* gene	This study
pRMPN8	pRMPN1 with L111I point mutation in the *wzy$_{Sf}$* gene	This study
pRMPN9	pRMPN1 with N86K point mutation in the *wzy$_{Sf}$* gene	This study
pRMPN10	pRMPN1 with L28V point mutation in the *wzy$_{Sf}$* gene	This study
pRMPN11	pRMPN1 with P165S point mutation in the *wzy$_{Sf}$* gene	This study
pRMPN12	pRMPN1 with G82C point mutation in the *wzy$_{Sf}$* gene	This study

TABLE 1 (Continued)

Strain or plasmid	Characteristics[a]	Reference or source
pRMPN13	pRMPN1 with N147K point mutation in the *wzy$_{Sf}$* gene	This study
pRMPN14	pRMPN1 with L191F point mutation in the *wzy$_{Sf}$* gene	This study
pRMPN15	pRMPN1 with L214I point mutation in the *wzy$_{Sf}$* gene	This study
pRMPN16	pRMPN1 with P352H point mutation in the *wzy$_{Sf}$* gene	This study
pRMPN17	pRMPN1 with V92 M point mutation in the *wzy$_{Sf}$* gene	This study
pRMPN19	pRMPN1 with F52Y point mutation in the *wzy$_{Sf}$* gene	This study
pRMPN21	pRMPN1 with F52C/I242T point mutations in the *wzy$_{Sf}$* gene	This study
pRMPN22	pRMPN1 with C60F point mutation in the *wzy$_{Sf}$* gene	This study
pRMPN23	pRMPN1 with Y137H point mutation in the *wzy$_{Sf}$* gene	This study
pRMPN24	pRMPN1 with L49F/T328A point mutation in the *wzy$_{Sf}$* gene	This study
pRMPN25	pRMPN1 with F54C point mutation in the *wzy$_{Sf}$* gene	This study
pCACTUS	Suicide vector containing *sacB*, Cm^r gene, and *ori$_{ts}$*	14
pRMA577	Suicide vector containing SphI-SphI fragment with the *rol* gene	14
pCACTUS-*wzz$_{Sf}$*::Tc^r	Suicide mutagenesis construct to construct the strain RMA4337	This study

[a] Rif^r, rifampin resistant; Km^r, kanamycin resistant; Cm^r, chloramphenicol resistant; Tet^r, tetracycline resistant. The λ DE3 genotype is λ sBamHIo ΔEcoRI-B *int*::(*lacI*::*PlacUV5*::T7 gene 1) *i21*.

150 mM NaCl, pH 7.5). The mixture was then lysed by sonication, followed by centrifugation (2,200 × *g*; Sigma 3K15 tabletop centrifuge; 10 min; 4°C) to remove debris. Ultracentrifugation was performed in a Beckman Coulter Optima MAX-XP tabletop ultracentrifuge (126,000 × *g* for 1 h at 4°C) to isolate the whole-membrane (WM) fraction. The WM fraction was resuspended in PBS and then solubilized in buffer A. The solubilized WM fraction from 3 × 10^8 cells was electrophoresed on an SDS–15% PAGE gel. The gel was rinsed with distilled water, and in-gel imaging was performed as described above. Loading was checked by staining the gel with Coomassie blue R-250. The intensity of Wzy$_{Sf}$-GFP expression for mutant and control strains was measured with the Fiji image-processing package (http://fiji.sc/Fiji), and the percent relative Wzy$_{Sf}$-GFP intensity for each mutant strain was measured by comparing the Wzy$_{Sf}$-GFP intensity of each mutant strain with the Wzy$_{Sf}$-GFP intensity in the control strain, PNRM13.

Colicin sensitivity assay. For the colicin sensitivity assay, a solution of purified His$_6$-ColE2 (ColE2) with an initial concentration of 1 mg/ml was used (11).

ColE2 swab assay. A 2-fold serial dilution of 1 μg/ml of ColE2 was swabbed onto antibiotic-selective LB agar plates containing 0.2% (wt/vol) L-arabinose with a cotton swab. The plates were left to dry for 1 h at room temperature (RT). Individual 0.2% (wt/vol) L-arabinose-induced mutant and control LB cultures were then swabbed perpendicular to the ColE2 streak, and the plates were left to dry for another 1 h at RT. The plates were then incubated for 16 h at 37°C. The susceptibilities of the mutant strains compared to the control strain were recorded, and images were taken using a Canon scanner (CanoScan 9000F) against a dark background.

ColE2 spot assay. A spot assay was performed using the serial dilutions of ColE2. One hundred microliters of the individual L-arabinose-induced mutant and control strain cultures were spread onto LB agar plates with appropriate antibiotics and 0.2% (wt/vol) L-arabinose. The plates were left to dry for 2 h at RT. A 2-fold serial dilution of 1 μg/ml of ColE2 (denoted neat [N]) was spotted on the dried plates, and the plates were left to dry for another 3 h at RT. The plates were then incubated for 18 h at 37°C. The endpoints of the killing zones of mutant strains were compared with the controls. Images were recorded as described above.

Bacteriophage sensitivity assay. The procedures of phage propagation and phage stock preparation have been described previously (3, 33). The concentration of the bacteriophage Sf6c stock used was 8.6 × 10^7 PFU/ml. Mutant and control strains were grown and induced with 0.2% (wt/vol) L-arabinose, and 100 μl of the individual mutant and control LB cultures was spread onto LB agar plates with appropriate antibiotics and 0.2% (wt/vol) L-arabinose. The plates were left to dry for 2 h at RT. Serial dilutions of the bacteriophage Sf6c stock (undiluted bacteriophage Sf6c stock was denoted N) were spotted on the dried plates, and the plates were

dried for a further 3 h at RT. The plates were incubated for 18 h at 37°C. The phage sensitivities of the test strains were compared with the controls. Images were recorded as described above.

RESULTS

Construction of a Wzy$_{Sf}$-GFP expression plasmid. A suitable expression system was constructed to express *wzy$_{Sf}$* and to detect Wzy$_{Sf}$ by fusion to GFP (29). *S. flexneri* 2457T 2a *wzy$_{Sf}$* with three modified codons at postions 4, 9, and 23 in the pRMCD6 plasmid (18) was PCR amplified and ligated into pWaldo-TEV-GFP (Table 1) (see Materials and Methods). To confirm that the construct was able to express the Wzy$_{Sf}$-GFP-His$_8$ protein, pWaldo-*wzy$_{Sf}$*-TEV-GFP-His$_8$ (denoted pRMPN1) was transformed into Lemo21(DE3) cells. Whole-cell in-gel fluorescence samples were then prepared from PNRM15 [Lemo21(DE3)(pRMPN1)], and fluorescence imaging of the gel detected a fluorescent band at approximately 64 kDa, which corresponded to the predicted size of the Wzy$_{Sf}$-GFP protein (see Fig. S1, lane 1, in the supplemental material), indicating that the construct was able to express Wzy$_{Sf}$-GFP.

Complementation of *wzy$_{Sf}$* deficiency. A complementation assay was performed to confirm the functionality of Wzy$_{Sf}$-GFP. For this assay, pRMPN1 was cotransformed, along with pAC/pBADT7-1 (34), into the *wzy$_{Sf}$*-deficient strain RMM109 (3). RMM109 has a frameshift mutation at position 9214 in the *wzy$_{Sf}$* gene that results in premature termination of Wzy$_{Sf}$ synthesis (3). pAC/pBADT7-1 encodes T7 RNA polymerase, which drives the expression of *wzy$_{Sf}$-gfp* in pRMPN1. LPS samples were prepared from these control strains. The silver-stained gel showed that PNRM6 [RMM109(pAC/pBADT7-1)] had an SR-LPS profile (Fig. 1, lane 3), but PNRM13 [PNRM6(pRMPN1)] had an S-LPS profile (Fig. 1, lane 5). Hence, pRMPN1 was able to complement the *wzy$_{Sf}$* mutation in RMM109, and the LPS profile resembled that of the wild-type strain PE638 (Fig. 1, lane 2).

Random mutagenesis of *wzy$_{Sf}$*. Nothing is known about the residues important for Wzy$_{Sf}$ function, and there is little sequence identity between the Wzy proteins of different bacterial species. Hence, it is difficult to predict the functional amino acid residues of the *S. flexneri* Wzy$_{Sf}$. To obtain insight into the Wzy$_{Sf}$ residues needed for function, the *wzy$_{Sf}$* coding region in plasmid pRMPN1 was subjected to random mutagenesis using an error-prone DNA
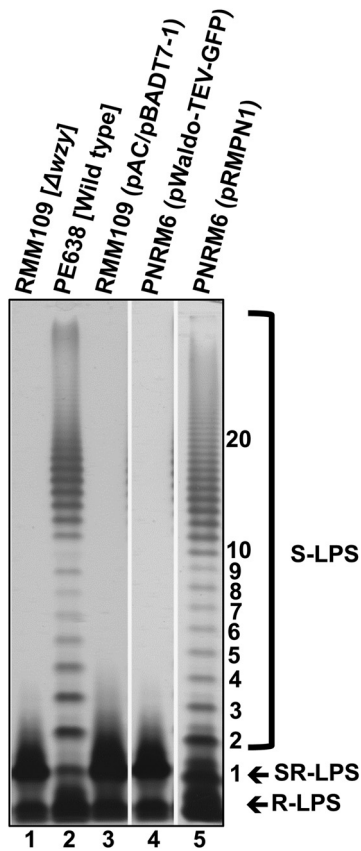
FIG 1 Complementation of *wzy*$_{Sf}$ deficiency by Wzy$_{Sf}$-GFP. LPS samples (equivalent to 1×10^9 bacterial cells) were prepared from the indicated strains by proteinase K treatment, electrophoresed on an SDS–15% (wt/vol) PAGE gel, and silver stained (see Materials and Methods). The positions of S-LPS, SR-LPS, and R-LPS are indicated. The numbers on the right indicate the Oag RUs.

polymerase (see Materials and Methods). The resulting mutagenized plasmid library was transformed into PNRM6. We screened the transformants to find mutants, using ColE2. The basis for this is that the R-LPS strains are more susceptible to killing by colicins than the S-LPS strains (12), and we recently found that there is a strong correlation between LPS Oag modal chain length and susceptibility to ColE2 (11). A ColE2 swab assay (see Materials and Methods) was used to screen and detect mutants that had different sensitivity to ColE2 than the positive-control strain PNRM13 (see Table S2 in the supplemental material). Interestingly the wild-type strain PE638 was slightly more resistant to ColE2 than the complemented positive-control strain PNRM13 (Table 2; see Table S2 in the supplemental material). The *wzy*$_{Sf}$ mutant RMM109 (SR-LPS) was highly sensitive to ColE2 (Table 2; see Table S2 in the supplemental material). Transformants that were either more resistant or more sensitive to ColE2 than PNRM13 were selected (see Table S2 in the supplemental material), and the plasmids were isolated and transformed into the XL10G strain. Plasmid DNA from these isolates was subjected to DNA sequencing to identify mutational alterations in *wzy*$_{Sf}$. The *wzy*$_{Sf}$ mutants had the following substitutions: P352H, V92M, Y137H, L214I, G130V, N147K, P165S, L191F, C60F, L49F/ T328A, L28V, N86K, F54C, F52Y, L111I, G82C, and F52C/I242T

(see Table S3 in the supplemental material). The mutations were present in PL1, PL2, PL3, and PL6, TM2, TM4, TM5, TM7, TM8, and TM9, and cytoplasmic loop 1 (CL1) and CL5 of the Wzy$_{Sf}$ topology map (summarized in Fig. 2 and Table 2). After sequence confirmation, the mutated plasmids were transformed into PNRM6 (Table 1) for detailed characterization.

LPS phenotype conferred by Wzy$_{Sf}$ mutants. The effects of mutations on Wzy$_{Sf}$ LPS Oag polymerization activity were determined by SDS-PAGE and silver staining. Following comparison of the resulting degree of LPS Oag polymerization of the mutant strains with the relevant positive control, PNRM13, the mutants were grouped into four different phenotypic classes: A, B, C, and D (Fig. 3; see Fig. S2 in the supplemental material). Three of the 17 mutants had reduced degrees of polymerization compared to PNRM13 and were classified as class A. Class A mutants had the following alterations in Wzy$_{Sf}$: P352H (WzyP352H), V92M (WzyV92M), and Y137H (WzyY137H) (Fig. 3, lanes 2 to 4). One mutant (with an L214I alteration in Wzy$_{Sf}$ [WzyL214I]) exhibited an LPS banding pattern with only a few Oag RUs and was classified as class B (Fig. 3, lane 5). Another mutant had SR-LPS (with a G130V alteration in Wzy$_{Sf}$ [WzyG130V]) and was categorized into class C (Fig. 3, lane 6). The other 12 mutations conferred an LPS profile similar to that of the positive control, PNRM13, and were classified as class D. Members of this class had the following mutations: N147K (WzyN147K), P165S (WzyP165S), L191F (WzyL191F), C60F (WzyC60F), L49F/T328A (WzyL49F/T328A), L28V (WzyL28V), N86K (WzyN86K), F54C (WzyF54C), F52Y (WzyF52Y), L111I (WzyL111I), G82C (WzyG82C), and F52C/ I242T (WzyF52C/I242T) (Fig. 3, lanes 7 to 10; see Fig. S2, lanes 1 to 8, in the supplemental material). Here, the mutant Wzy$_{Sf}$ proteins are referred to according to their conferred LPS classes.

Wzz$_{Sf}$ dependence. Since the Wzy-dependent model of LPS assembly suggests a potential interaction between Wzy and Wzz, we investigated if the LPS profile conferred by mutated Wzy$_{Sf}$ proteins was dependent on the presence of Wzz$_{Sf}$. All the plasmids encoding mutated Wzy$_{Sf}$ proteins were transformed into RMA4337 carrying pAC/pBADT7-1 (strain PNRM126) (Table 1). RMA4337 is a *wzy*$_{Sf}$ and *wzz*$_{Sf}$ double mutant. The LPS profiles conferred in the PNRM126 background (Δ*wzy* Δ*wzz*) were directly compared with the LPS profile conferred in the Δ*wzy* background (PNRM6). The control strain PNRM134 [PNRM126(pRMPN1)] had S-LPS without Oag modal chain length control (Fig. 4, lane 3), as expected, and was classified as class E for the purpose of comparison. PNRM126 with mutated *wzy*$_{Sf}$ plasmids that conferred a class A LPS profile in the Δ*wzy* background had a class E LPS profile similar to that of PNRM134, except that PNRM126 expressing WzyP352H had LPS with few Oag RUs (class B) (Fig. 4, lane 5). PNRM126 expressing WzyL214I had SR-LPS (Fig. 4, lane 11). However, in comparison, PNRM6 (Δ*wzy*) expressing WzyL214I conferred a class B LPS profile (Fig. 4, lane 10). PNRM126 with a mutated *wzy*$_{Sf}$ plasmid that conferred a class C LPS profile in the Δ*wzy* background (PNRM6 expressing G130V) had S-LPS without modal length control and a reduced degree of polymerization (designated class F) compared to PNRM134 (Fig. 4, lane 13). PNRM126 with mutated *wzy*$_{Sf}$ plasmids from the strains with a class D LPS profile in the Δ*wzy* background had a class E LPS profile, similar to that of PNRM134 (Fig. 4, lanes 14 to 21; see Fig. S3, lanes 1 to 16, in the supplemental material). Hence, certain Wzy$_{Sf}$ mutants conferred dramatically

TABLE 2 ColE2 and bacteriophage Sf6c sensitivities and Wzy$_{Sf}$-GFP expression of controls and different classes of mutants

Strain or mutant	Relevant detail(s)	Mutant class Δwzy background	Mutant class ΔwzyΔwzz background	Topology map location[a]	ColE2 Δwzy background	ColE2 ΔwzyΔwzz background	Sf6c Δwzy background	Sf6c ΔwzyΔwzz background	Relative Wzy$_{Sf}$-GFP expression (%) Δwzy background	Relative Wzy$_{Sf}$-GFP expression (%) ΔwzyΔwzz background
Strains										
RMM109	wzy$_{Sf}$ mutants				1/256		R			
PE638	Wild type				R		10^{-6}			
PNRM13	Positive control				1/2		10^{-5}		100	
PNRM6	Negative control				1/256		R			
PNRM11	Negative control				1/256		R			
RMA4337	wzy$_{Sf}$ and wzz$_{Sf}$ mutant					1/256		R		
PNRM126	Negative control					1/256		R		
PNRM134	Positive control					R		10^{-6}		17
Mutants										
P352H		A	B	PL6	1/64	1/128		R	36	38
V92M		A	E	PL2	1/32	1/64		R	84	76
Y137H		A	E	TM5	1/32	1/64		R	87	97
L214I		B	C	TM8	1/128	1/128		R	1.4	0.03
G130V		C	F	TM5	1/512	1/128		R	1.60	28.50
N147K		D	E	PL3	R	1/16		R	21	52
P165S		D	E	PL3	1/4	1/64		N	7	125
L191F		D	E	TM7	R	1/16		N	162	64
C60F		D	E	TM1	R	1/64		N	30	66
L49F/T328A		D	E	TM2/CL5	R	1/64		R	65	68
L28V		D	E	PL1	R	1/8		N	55	80
N86K		D	E	PL2	R	1/64		N	84	82
F54C		D	E	CL1	R	1/64		R	42	71
F52Y		D	E	TM2	R	1/64		R	47	63
L111I		D	E	TM4	R	1/8		N	41	51
G82C		D	E	PL2	R	1/64		R	40	47
F52C/I242T		D	E	TM2/TM9	R	1/64		N	82	81

[a] PL, periplasmic loop; TM, transmembrane region; CL, cytoplasmic loop (Fig. 2).

[b] R, resistant; N, plaques detected with undiluted Sf6c stock. The numbers indicate the highest dilution showing a zone of inhibition or plaque formation.
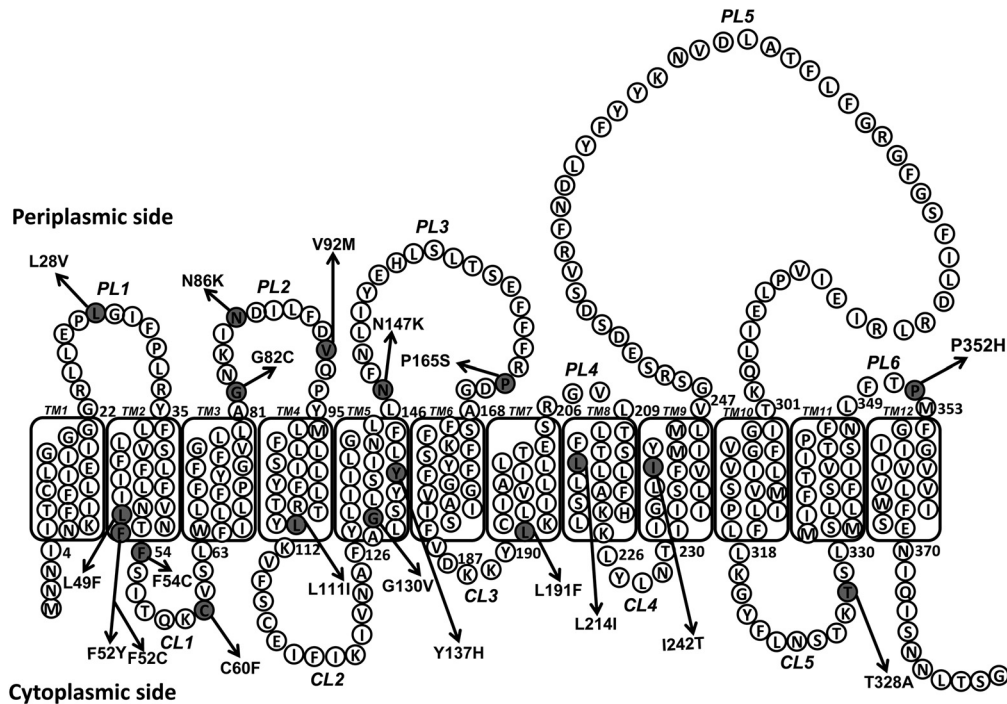
FIG 2 Locations of mutations on the topology map of Wzy$_{Sf}$. Mutational alterations are indicated by arrows on the Wzy$_{Sf}$ topology map (adapted from reference 18). The positions of the periplasmic loops (PL1 to PL5), transmembrane regions (TM1 to TM12), and cytoplasmic loops (CL1 to CL5) are indicated. Mutations (shaded circles) are located in PL1, PL2, PL3, and PL6, TM2, TM4, TM5, TM7, TM8, and TM9, and CL1 and CL5.

different LPS profiles depending on the presence or absence of Wzz$_{Sf}$.

ColE2 and bacteriophage Sf6c sensitivities. To confirm the LPS profiles determined as described above using assays of LPS Oag function, the ColE2 and bacteriophage Sf6c sensitivities of the mutant strains were investigated. ColE2 sensitivity (summarized in Table 2) was determined by spot testing, as described in Materials and Methods. Strains RMM109, PNRM6, PNRM11, RMA4337, and PNRM126 showed killing zones at a dilution of 1/256. The wild-type strain PE638 was resistant to the highest concentration of ColE2 used. The relevant positive-control strain in the Δ*wzy* background (PNRM13) showed a killing zone at a dilution of 1/2, but the relevant positive-control strain in the Δ*wzy* Δ*wzz* background (PNRM134) was resistant to the highest concentration of ColE2 tested. Strains conferring a class A LPS profile in the Δ*wzy* background were sensitive to ColE2 (killing zone at 1/32 or 1/64). However, Δ*wzy* Δ*wzz* strains with mutated *wzy*$_{Sf}$ plasmids conferring the class A LPS profile in the Δ*wzy* background were 2-fold more sensitive to ColE2 (killing zone at 1/64 or 1/128) than the Δ*wzy* background. The Δ*wzy* strain expressing WzyL214I (class B) and the Δ*wzy* Δ*wzz* strain expressing WzyL214I (class C) had similar ColE2 sensitivities (1/128). The strain with the class C LPS profile (Δ*wzy* expressing WzyG130V) had the greatest sensitivity to ColE2 (1/512), greater than RMM109 and the negative-control strains (PNRM6, PNRM11, and PNRM126). However, the Δ*wzy* Δ*wzz* strain expressing WzyG130V (class F) was more resistant (1/128) to ColE2 than the Δ*wzy* background. Strains with a class D LPS profile in the Δ*wzy* background were resistant to the highest concentration of ColE2 tested, except that Δ*wzy* expressing WzyP165S showed slight sensitivity (1/4). Hence, almost all the strains with a class D LPS

profile in the Δ*wzy* background were more resistant to ColE2 than PNRM13 and were similar to PE638. The Δ*wzy* Δ*wzz* strains with mutated *wzy*$_{Sf}$ plasmids from the strains with a class D LPS profile in the Δ*wzy* background were more sensitive to ColE2 (killing zone at 1/8 to 1/64) than the control, PNRM134 [Δ*wzy* Δ*wzz*(pRMPN1)], suggesting they have a slight defect in Oag polymerization in the absence of Wzz$_{Sf}$. Hence, ColE2 resistance correlated with the degree of Oag polymerization and the degree of LPS capping with Oag.

The bacteriophage Sf6c sensitivities of the strains carrying mutated *wzy*$_{Sf}$ plasmids (summarized in Table 2) were determined by spot testing, as described in Materials and Methods. The SR-LPS strains RMM109, PNRM6, PNRM11, RMA4337, and PNRM126 were resistant to bacteriophage Sf6c. The S-LPS strains, wild-type PE638, and the controls, PNRM13 and PNRM134, were bacteriophage Sf6c sensitive, and plaques were detected at 10^{-6}, 10^{-5}, and 10^{-6} dilutions, respectively. Strains with class A, B, and C LPS profiles in the Δ*wzy* background were resistant to the highest concentration of bacteriophage Sf6c tested and were similar to the strains with SR-LPS (RMM109, PNRM6, PNRM11, RMA4337, and PNRM126). Similarly, the Δ*wzy* Δ*wzz* strains with mutated *wzy*$_{Sf}$ plasmids from the strains with class A, B, and C LPS profiles in the Δ*wzy* background were also resistant to the highest concentration of bacteriophage Sf6c tested. Strains with a class D LPS profile in the Δ*wzy* background were bacteriophage Sf6c sensitive (plaques at 10^{-6}), except that the strain expressing WzyP165S was slightly less sensitive (plaque at 10^{-5}). Hence, the bacteriophage Sf6c sensitivities of the strains with a class D LPS profile in the Δ*wzy* background were greater than that of PNRM13 and similar to that of PE638. Δ*wzy* Δ*wzz* strains with mutated *wzy*$_{Sf}$ plasmids from the strains with a class D LPS profile in the Δ*wzy* background
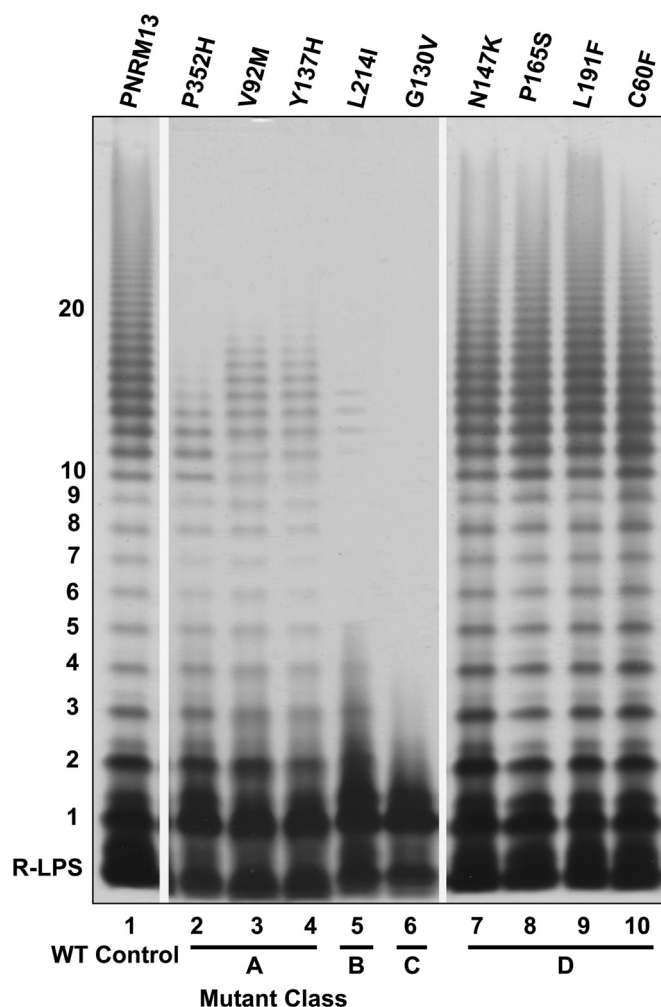
FIG 3 LPS phenotypes conferred by different Wzy$_{Sf}$ mutants expressed in PNRM6 [Δ*wzy$_{Sf}$*(pAC/pBADT7-1)]. Plasmid-encoded mutated Wzy$_{Sf}$ proteins were expressed in PNRM6. The strains were grown and induced with arabinose as described in Materials and Methods. LPS samples were prepared, electrophoresed on SDS–15% (wt/vol) PAGE gels, and silver stained (see Materials and Methods). The strains were divided into various mutant classes (A, B, C, and D) based on their LPS phenotypes. Lane 1, positive-control strain PNRM13 [PNRM6(pRMPN1)]; lanes 2 to 10, Δ*wzy* strain (PNRM6) with plasmids encoding mutated Wzy$_{Sf}$ proteins, as indicated. The position of R-LPS is indicated. The numbers on the left indicate the Oag RUs. WT, wild type.

were more resistant to bacteriophage Sf6c than the Δ*wzy* background. Although they have a class E LPS profile, similar to PNRM134, they were more resistant to bacteriophage Sf6c than PNRM134. Hence, bacteriophage Sf6c sensitivity correlated with the degree of Oag polymerization and the degree of LPS capping with Oag.

Wzy$_{Sf}$ expression level. We determined the levels of parental and mutant Wzy$_{Sf}$-GFP expressed in Δ*wzy* and Δ*wzy* Δ*wzz* *S. flexneri* strains. To measure the protein expression levels of the mutants, in-gel fluorescence testing was performed, and the percent relative Wzy$_{Sf}$-GFP expression was calculated (see Materials and Methods). The expression levels of different Wzy$_{Sf}$-GFP mutants were compared with that of Wzy$_{Sf}$-GFP in PNRM13 (100%). The Wzy$_{Sf}$-GFP expression level in PNRM134 was less than that in PNRM13 (Fig. 5A and B, lane 2), with a relative Wzy$_{Sf}$-GFP level

of 17% (Table 2). In the Δ*wzy* background, the Wzy$_{Sf}$-GFP mutants were expressed at a level less than 100%, except the L191F mutant (class D), which had expression of 162% (Fig. 5B, lane 7, and Table 2). However, in the Δ*wzy* Δ*wzz* background, the relative Wzy$_{Sf}$-GFP level of the L191F mutant was 64% (Fig. 5B, lane 8, and Table 2), which was less than the control strain, PNRM13. In the Δ*wzy* background, the relative Wzy$_{Sf}$-GFP levels of P165S, L214I, and G130V mutants were very low (7%, 1.4%, and 1.6%, respectively) (Fig. 5B, lane 5, and A, lanes 9 and 11, and Table 2). However, in the Δ*wzy* Δ*wzz* background, P165S and G130V mutants had relative Wzy$_{Sf}$-GFP levels of 125% and 28.50%, respectively (Fig. 5B, lane 6, and A, lane 12, and Table 2), but the relative Wzy$_{Sf}$-GFP level of the L214I mutant was almost undetectable at 0.03% (Fig. 5A, lane 10, and Table 2). In the Δ*wzy* Δ*wzz* background, the relative Wzy$_{Sf}$-GFP level of the P165S mutant was higher than that of the control, PNRM13 (100%) (Fig. 5B, lane 6, and Table 2). These data indicate that expression of certain Wzy$_{Sf}$ mutants was affected by Wzz$_{Sf}$ but that the effect was mutant specific.

DISCUSSION

In this study, we constructed and characterized a collection of *wzy$_{Sf}$* mutants. We found that ColE2 screening was an effective method to detect *wzy$_{Sf}$* mutants conferring subtle effects on LPS structure (Table 2). The use of Wzy$_{Sf}$-GFP allowed comparison of the protein expression levels of different mutants. We also found that bacteriophage Sf6c sensitivity was dependent on the LPS phenotype structure. Strains with mutant Wzy$_{Sf}$ conferring a longer Oag chain and/or a greater degree of Oag polymerization were more sensitive to bacteriophage Sf6c, while bacteriophage Sf6c infected only strains with wild-type (or nearly wild-type) LPS, both in the degree of Oag polymerization and the apparent level of LPS capping with Oag chains.

Only a few studies have been conducted on Wzy proteins. During characterization of Wzy of *Francisella tularensis*, Kim et al. reported several amino acid residues important for Oag polymerization. Modification of these residues (G176, D177, G323, and Y324) led to a loss of Oag polymerization [35]. Islam et al. showed that PL3 and PL5 of Wzy$_{Pa}$ have net positive and net negative charges, respectively, and they established their "catch-and-release" model [20]. However, for Wzy$_{Sf}$, we found that at a physiological pH both PL3 and PL5 possess net negative charges (the pI of PL3 is 4.65, and that of PL5 is 5.09). In *Pseudomonas aeruginosa* PAO1 there is a uronic acid sugar in the Oag [36] that is negatively charged. However, the Oag of Wzy$_{Sf}$ is neutral. Therefore, the charge property of the substrate for Wzy$_{Sf}$ is different from that of Wzy$_{Pa}$. The RX$_{10}$G motifs of PL3 and PL5 of Wzy$_{Pa}$ [20] are also absent in Wzy$_{Sf}$. However, both PL3 and PL5 of Wzy$_{Sf}$ contained RX$_{15}$G motifs (starting from R164 in PL3 and R289 in PL5) (Fig. 2). Therefore, perhaps a modified version of the "catch-and-release" mechanism [20] exists for *S. flexneri*. Moreover, addition of either glucosyl or *O*-acetyl groups or PEtN residues by various linkages to the sugars within the tetrasaccharide repeats of serotype Y creates 17 different serotypes of *S. flexneri* [5–7]. As the polymerization of all these Oags is done by Wzy$_{Sf}$, we conclude that Wzy$_{Sf}$ must be quite flexible in its substrate recruitment. Due to scant homology between *wzy* proteins of different bacterial species, we were unable to create any directly comparable mutation in Wzy$_{Sf}$ with respect to other systems. This led us to perform random mutagenesis on *wzy$_{Sf}$*, followed by screening with ColE2.
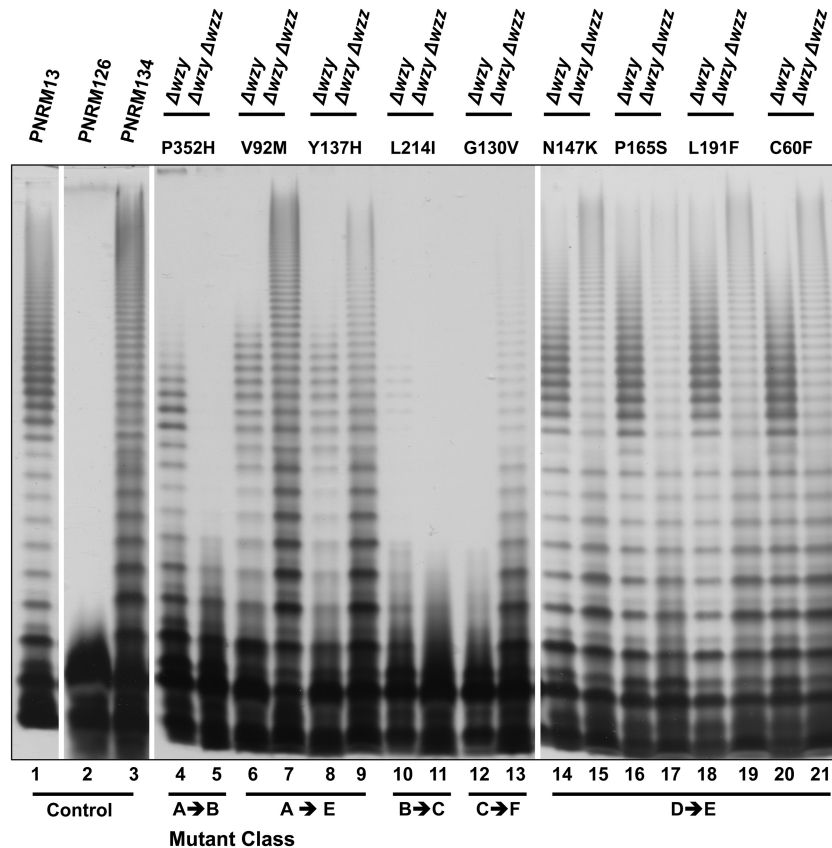
FIG 4 Comparison of the LPS phenotypes conferred by the Wzy_Sf mutants expressed in the Δ*wzy* and Δ*wzy* Δ*wzz* backgrounds. Plasmids encoding mutated Wzy_Sf proteins were expressed in PNRM126 [RMA4337(pAC/pBADT7-1)] and PNRM6 [RMM109(pAC/pBADT7-1)]. The strains were grown and induced as described in Materials and Methods. LPS samples were electrophoresed on SDS–15% (wt/vol) PAGE gels and silver stained (see Materials and Methods). Lanes 1 to 3 contain the indicated strains; lanes 4 to 21 contain the Δ*wzy* (PNRM6) or Δ*wzy* Δ*wzz* (PNRM126) strain with plasmids encoding the indicated mutated Wzy_Sf proteins.

The mutations we found are present in a wide region (PL1, PL2, PL3, and PL6, TM2, TM4, TM5, TM7, TM8, and TM9, and CL1 and CL5) of the Wzy_Sf topological model experimentally determined by Daniels et al. (18). We were able to locate a number of mutations in the TM regions, and interestingly, the G130V mutation, which resulted in the complete loss of polymerization activity of Wzy_Sf in the Δ*wzy* background, was also located in TM5. Topological models are not very accurate, but due to a lack of crystal structure, we used the Wzy_Sf topology model previously determined by our group to locate the mutational alterations. Furthermore, we reassessed our topological model using 5 different topology prediction programs (SPOCTOPUS, MEMSAT, HMMTOP, TOPCONS, and TMHMM) (see Table S4 in the supplemental material). The results showed that until TM region 6, all the programs are consistent with our topological model. Three of them also validate TM10 to TM11 of our topological model. Thus, the topological model of Wzy_Sf determined by our group is nearly consistent with the topological models predicted by the programs. The mutations that resulted in the partial loss of polymerization in the Δ*wzy* background were V92M, Y137H, L214I, and P352H. Among them, V92M and Y137H are present in PL2 and TM5. These regions were validated by all 5 of the programs. P352H is present in PL6, and the region was validated by 3 of the programs (MEMSAT, HMMTOP, and TOPCONS). L214I is present in TM8, and the

region (amino acids 209 to 226) was different from the computer prediction (amino acids 227 to 247). However, G130V is present in TM5, which was validated by all 5 of the programs. Recently, Reddy et al. reported that different topology prediction programs are suitable for different families of proteins (37). Therefore, lack of prediction of TM7 to TM9 by some programs does not invalidate the presence of these regions in our model.

In the Δ*wzy* background, strains with the class A LPS profile had S-LPS with a reduced degree of Oag polymerization (Fig. 3, lanes 2 to 4), mutants with the class B LPS profile had LPS with few Oag RUs (Fig. 3, lane 5), and the mutant with a class C LPS profile had SR-LPS (Fig. 3, lane 6). As a result, the class A mutants were more sensitive to ColE2 than PNRM13, and the class B mutants were even more sensitive to ColE2 than the mutants with the class A LPS profile. The mutant with class C LPS had the highest ColE2 sensitivity. From these three classes, it is clear that the LPSs with shorter Oag chains were more sensitive to ColE2. Strains with Class A, B, and C LPS profiles in the Δ*wzy* background were resistant to bacteriophage Sf6c. The lack of bacteriophage Sf6c sensitivity indicates that bacteriophage Sf6c infects only if the LPS has a wild-type or close to a wild-type level of Oag polymerization. In this study, we found that the Wzy_Sf mutants conferring the class D LPS profile in the Δ*wzy* background had a level of Oag polymerization similar to that of the positive-control strain PNRM13, as
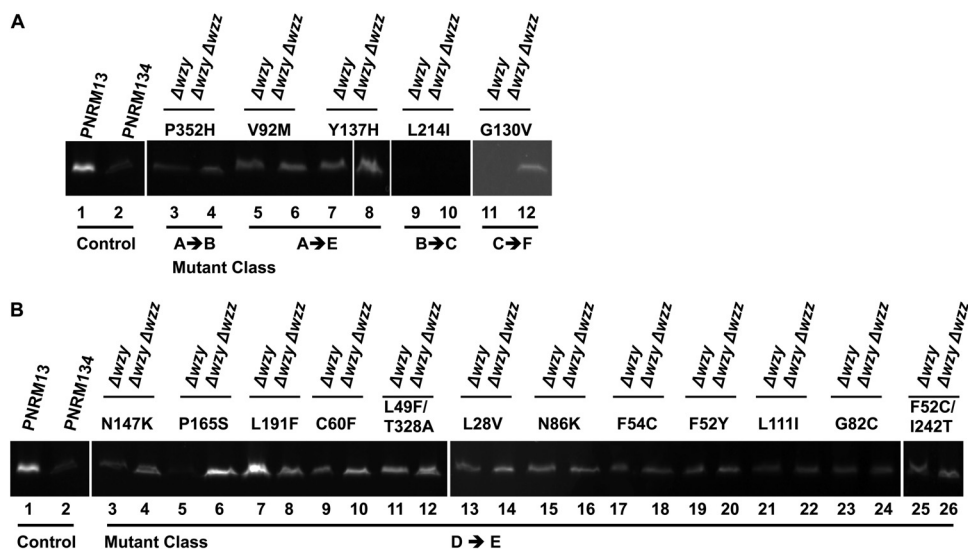
FIG 5 Protein expression levels of the mutated Wzy$_{Sf}$-GFP compared to the positive control. The strains were grown in LB and induced as described in Materials and Methods. In-gel fluorescence samples were prepared from the mutants in the Δ*wzy* and Δ*wzy* Δ*wzz* backgrounds and electrophoresed on SDS–15% (wt/vol) PAGE gels (see Materials and Methods). (A) Lanes 1 and 2 contain the indicated strains; lanes 3 to 12 contain the Δ*wzy* or Δ*wzy* Δ*wzz* strain expressing mutated Wzy$_{Sf}$-GFP, as indicated. (B) Lanes 1 and 2 contain the indicated strains; lanes 2 to 26 contain the Δ*wzy* or Δ*wzy* Δ*wzz* strain expressing mutated Wzy$_{Sf}$-GFP, as indicated.

determined by SDS-PAGE and silver staining (Fig. 3, lanes 7 to 10; see Fig. S2, lanes 1 to 8, in the supplemental material), but they were more resistant to ColE2 and more sensitive to bacteriophage Sf6c (Table 2) (except the Δ*wzy* strain with WzyP165S). The ColE2 and bacteriophage Sf6c sensitivities of these strains were similar to those of wild-type strain PE638. We conclude that the Oag polymerization activities of the mutants with a class D LPS profile in the Δ*wzy* background were similar to that of the wild-type strain (PE638). Hence, the wild-type Wzy$_{Sf}$-GFP protein is not 100% active, and the mutant proteins conferring the class D LPS profile are more active and/or are better exported, folded, or assembled to the IM. The levels of Oag polymerization of the strains with a class D LPS profile were more than that of PNRM13, although this was not distinguishable by silver staining. Hence, the ColE2 assay was more sensitive than silver staining and SDS-PAGE in determining the degree of Oag polymerization.

Mutation in *wzz* resulted in Oags without modal chain length control in different organisms (14, 24). Recently, Kenyon and Reeves showed that Wzy of *Yersinia pseudotuberculosis* also needs Wzz for complete Oag polymerization (38). Here, we examined the polymerization activities of different Wzy$_{Sf}$ mutants in the absence of Wzz$_{Sf}$. In the Δ*wzy* Δ*wzz* background, the strain with mutated *wzy$_{Sf}$* plasmids from the strain having class B LPS profiles in the Δ*wzy* background had an SR-LPS profile, and ColE2 and bacteriophage Sf6c sensitivities were similar to those in the Δ*wzy* background. Interestingly, the Δ*wzy* Δ*wzz* strain with WzyG130V had S-LPS without modal length control (class F), whereas the Δ*wzy* strain with WzyG130V had SR-LPS (class C), and this correlated with increased resistance to ColE2. In the Δ*wzy* Δ*wzz* background, strains with a class E LPS profile (S-LPS without modal length control) had increased sensitivity to ColE2 and increased or similar resistance to bacteriophage Sf6c compared to PNRM134 [Δ*wzy* Δ*wzz*(pRMPN1)] and the Δ*wzy* background (class A and class D) (Table 2). We speculate that these strains (strains with a class E LPS profile) had subtle alterations in the level of Oag po-

lymerization and/or capping of LPS with Oag and were unable to act efficiently as a bacteriophage Sf6c receptor and, correspondingly, were also more sensitive to ColE2. It is known that phage adsorption to the cells of *Escherichia coli* K-12 increases with an increase in the density of receptor protein at the cell surface (39). Based on our study, the relationship between ColE2 and the Oag density/concentration seems to be linear. Decreasing Oag progressively increases sensitivity to ColE2. However, the relationship between bacteriophage Sf6c and the Oag density/concentration seems to be nonlinear. Decreasing Oag rapidly decreases sensitivity to bacteriophage Sf6c. This may be because bacteriophage Sf6c interaction with its receptor is complex and most likely requires multireceptor binding to bacteriophage Sf6c tail spike proteins (TSPs) to achieve irreversible binding and hence activation of bacteriophage Sf6c.

According to the proposed molecular-clock model, Wzz acts as a molecular clock and regulates Wzy activity between two states: the E, or extension, state favors polymerization, and the T, or transfer, state favors the ligation reaction (24). The molecular-chaperone model describes Wzz as a typical molecular chaperone that regulates the overall ratio of Wzy and WaaL in a complex and controls the enzyme kinetics of the ligation reaction to define the modality (14). However, Woodward et al. suggested that there is an interaction between Wzy and Wzz, and they showed that the proteins are enough to shape the Oag modal chain length (26). Islam et al. suggested that the chain length of the Oag is determined by the interaction of Wzz and Wzy (40). Recent work of Taylor et al. also suggested the direct interaction of Wzz and Wzy in the Oag biosynthesis pathway (41). In this study, for the first time, we were able to provide insight into the association of Wzy$_{Sf}$ and Wzz$_{Sf}$ in Oag biosynthesis. We found Wzy$_{Sf}$ mutants in which polymerization activity was dependent on Wzz$_{Sf}$ (WzyP352H and WzyL214I) and some other mutants in which polymerization activity was repressed in the presence of Wzz$_{Sf}$ (WzyV92M, WzyY137H, and WzyG130V). The Δ*wzy* Δ*wzz* strains with

WzyV92M or WzyY137H had S-LPS without modal length control (class E), but in the Δ*wzy* background, they showed a class A LPS profile (a greatly reduced degree of Oag polymerization) (Fig. 4, lanes 6 and 7 and lanes 8 and 9). The Δ*wzy* strain with WzyG130V had a class C LPS profile (SR-LPS), but remarkably, the Δ*wzy* Δ*wzz* strain with WzyG130V had S-LPS without modal length control, albeit with a reduced degree of polymerization (class F) (Fig. 4, lanes 12 and 13). Oag polymerization by these Wzy$_{Sf}$ mutants was repressed by Wzz$_{Sf}$ in the Δ*wzy$_{Sf}$* background; their LPSs had shorter Oag chains. The Δ*wzy* strain with WzyP352H had a class A LPS profile, and the Δ*wzy* strain with WzyL214I had a class B LPS profile, but in the Δ*wzy* Δ*wzz* background they had shorter Oag chains (class B and C, respectively) than the Δ*wzy* background (Fig. 4, lanes 4 and 5 and lanes 10 and 11). Thus, these Wzy$_{Sf}$ mutants need Wzz$_{Sf}$ for their Oag polymerization activities. These findings suggest that Wzz$_{Sf}$ is associated with Wzy$_{Sf}$ not only for Oag modal chain length control but also for polymerization activity, and that the amino acids V92, G130, Y137, L214, and P352 have roles in the association of Wzy$_{Sf}$ and Wzz$_{Sf}$ during Oag polymerization mediated by Wzy$_{Sf}$.

The relative Wzy$_{Sf}$-GFP level in PNRM134 (Δ*wzy* Δ*wzz*) was lower than in PNRM13 (Δ*wzy*) (Fig. 5A and B, lanes 1 and 2), suggesting that the wild-type Wzy$_{Sf}$-GFP had better expression in the presence of Wzz$_{Sf}$. Wzy$_{Sf}$ mutants conferring a class A LPS profile (Δ*wzy* background) had Wzy$_{Sf}$-GFP levels lower than that of Wzy$_{Sf}$-GFP in PNRM13 (Fig. 5A, lanes 3, 5, and 7, and Table 2). WzyL214I was not detectable in either the Δ*wzy* (class B) or the Δ*wzy* Δ*wzz* (class C) background (Fig. 5A, lanes 9 and 10, and Table 2). Hence, amino acid L214 is important for Wzy$_{Sf}$-GFP production. WzyG130V was not detectable in the Δ*wzy* background (class C) but was detected in the Δ*wzy* Δ*wzz* background (class F) (Fig. 5A, lanes 11 and 12, and Table 2). Except for the Δ*wzy* strain with WzyL191F, all the mutants with a class D LPS profile (Δ*wzy* background) had protein expression levels lower than that of Wzy$_{Sf}$-GFP in PNRM13 (Fig. 5B and Table 2) by some unknown mechanism. However, the mutants with a class D LPS profile (Δ*wzy* background) had S-LPS and were more resistant to ColE2 and more sensitive to bacteriophage Sf6c than PNRM13. In the Δ*wzy* Δ*wzz* background, WzyL191F had an expression level lower than that of Wzy$_{Sf}$-GFP in PNRM13 (Fig. 5B, lane 8, and Table 2). WzyP165S was not detectable in PNRM6 (Δ*wzy*), but strain PNRM126 (Δ*wzy* Δ*wzz*) had WzyP165S present at a higher level than Wzy$_{Sf}$-GFP in PNRM13 (Fig. 5B, lanes 5 and 6, and Table 2). Apparently, there is more than one underlying mechanism for the class D (Δ*wzy* background) to class E (Δ*wzy* Δ*wzz* background) LPS profile conversion. Two of the mutations (P165S and G130V) resulted in decreased Wzy$_{Sf}$-GFP levels in the presence of Wzz$_{Sf}$. This suggested that the presence of Wzz$_{Sf}$ destabilizes WzyP165S and WzyG130V, which results in lower Wzy$_{Sf}$-GFP levels. The mutation L191F resulted in decreased Wzy$_{Sf}$-GFP levels in the absence of Wzz$_{Sf}$. Therefore, in this case, Wzz$_{Sf}$ stabilizes the protein WzyL191F, resulting in better Wzy$_{Sf}$-GFP expression. This finding suggests that G130, P165, and L191 are important for the stabilization of Wzy$_{Sf}$ through interaction with Wzz$_{Sf}$.

In conclusion, our findings identified amino acid residues on Wzy$_{Sf}$ important for its polymerization function and interaction with Wzz$_{Sf}$. Residues that are important for the polymerization and interaction of Wzz$_{Sf}$ and Wzy$_{Sf}$ are present in PL2 and PL6 and TM5 and TM8. These regions may contribute to the interaction of Wzy$_{Sf}$ with substrates and also to the interaction with Wzz$_{Sf}$. We identified a number of amino acids (G130, P165, and L191) that are important for the stabilization of Wzy$_{Sf}$ in association with Wzz$_{Sf}$. Hence, our data suggested that Wzz$_{Sf}$ also has a role in Wzy$_{Sf}$ stability.

REFERENCES

1. **Sperandeo P, Deho G, Polissi A.** 2009. The lipopolysaccharide transport system of Gram-negative bacteria. Biochim Biophys Acta **1791:**594–602. http://dx.doi.org/10.1016/j.bbalip.2009.01.011.

2. **Raetz CR, Whitfield C.** 2002. Lipopolysaccharide endotoxins. Annu Rev Biochem **71:**635–700. http://dx.doi.org/10.1146/annurev.biochem.71.110601.135414.

3. **Morona R, Mavris M, Fallarino A, Manning PA.** 1994. Characterization of the *rfc* region of *Shigella flexneri.* J Bacteriol **176:**733–747.

4. **Sun Q, Lan R, Wang Y, Wang J, Wang Y, Li P, Du P, Xu J.** 2013. Isolation and genomic characterization of SfI, a serotype-converting bacteriophage of *Shigella flexneri.* BMC Microbiol **13:**39. http://dx.doi.org/10.1186/1471-2180-13-39.

5. **Wang X, Zhang C, Shi F, Hu X.** 2010. Purification and characterization of lipopolysaccharides. Subcell Biochem **53:**27–51. http://dx.doi.org/10.1007/978-90-481-9078-2_2.

6. **Allison GE, Verma NK.** 2000. Serotype-converting bacteriophages and O-antigen modification in *Shigella flexneri.* Trends Microbiol **8:**17–23. http://dx.doi.org/10.1016/S0966-842X(99)01646-7.

7. **Sun Q, Knirel YA, Lan R, Wang J, Senchenkova SN, Jin D, Shashkov AS, Xia S, Perepelov AV, Chen Q, Wang Y, Wang H, Xu J.** 2012. A novel plasmid-encoded serotype conversion mechanism through addition of phosphoethanolamine to the O-antigen of *Shigella flexneri.* PLoS One **7:**e46095. http://dx.doi.org/10.1371/journal.pone.0046095.

8. **Jennison AV, Verma NK.** 2004. *Shigella flexneri* infection: pathogenesis and vaccine development. FEMS Microbiol Rev **28:**43–58. http://dx.doi.org/10.1016/j.femsre.2003.07.002.

9. **Stagg RM, Tang SS, Carlin NI, Talukder KA, Cam PD, Verma NK.** 2009. A novel glucosyltransferase involved in O-antigen modification of *Shigella flexneri* serotype 1c. J Bacteriol **191:**6612–6617. http://dx.doi.org/10.1128/JB.00628-09.

10. **Hong M, Payne SM.** 1997. Effect of mutations in *Shigella flexneri* chromosomal and plasmid-encoded lipopolysaccharide genes on invasion and serum resistance. Mol Microbiol **24:**779–791. http://dx.doi.org/10.1046/j.1365-2958.1997.3731744.x.

11. **Tran EN, Papadopoulos M, Morona R.** 2014. Relationship between O-antigen chain length and resistance to colicin E2 in *Shigella flexneri.* Microbiology **160:**589–601. http://dx.doi.org/10.1099/mic.0.074955-0.

12. **van der Ley P, de Graaff P, Tommassen J.** 1986. Shielding of *Escherichia coli* outer membrane proteins as receptors for bacteriophages and colicins by O-antigenic chains of lipopolysaccharide. J Bacteriol **168:**449–451.

13. **Lindberg AA, Wollin R, Gemski P, Wohlhieter JA.** 1978. Interaction between bacteriophage Sf6 and *Shigella flexneri.* J Virol **27:**38–44.

14. **Morona R, van den Bosch L, Manning PA.** 1995. Molecular, genetic, and topological characterization of O-antigen chain length regulation in *Shigella flexneri.* J Bacteriol **177:**1059–1068.

15. **Liu D, Cole RA, Reeves PR.** 1996. An O-antigen processing function for Wzx (RfbX): a promising candidate for O-unit flippase. J Bacteriol **178:**2102–2107.

16. **Guo H, Yi W, Song J K, Wang PG.** 2008. Current understanding on biosynthesis of microbial polysaccharides. Curr Top Med Chem **8:**141–151. http://dx.doi.org/10.2174/156802608783378873.

17. **Macpherson DF, Manning PA, Morona R.** 1995. Genetic analysis of the *rfbX* gene of *Shigella flexneri.* Gene **155:**9–17. http://dx.doi.org/10.1016/0378-1119(94)00918-I.

18. **Daniels C, Vindurampulle C, Morona R.** 1998. Overexpression and topology of the *Shigella flexneri* O-antigen polymerase (Rfc/Wzy). Mol Microbiol **28:**1211–1222. http://dx.doi.org/10.1046/j.1365-2958.1998.00884.x.

19. **Ruiz N, Gronenberg LS, Kahne D, Silhavy TJ.** 2008. Identification of two inner-membrane proteins required for the transport of lipopolysaccharide to the outer membrane of *Escherichia coli*. Proc Natl Acad Sci U S A **105**:5537–5542. http://dx.doi.org/10.1073/pnas.0801196105.

20. **Islam ST, Gold AC, Taylor VL, Anderson EM, Ford RC, Lam JS.** 2011. Dual conserved periplasmic loops possess essential charge characteristics that support a catch-and-release mechanism of O-antigen polymerization by Wzy in *Pseudomonas aeruginosa* PAO1. J Biol Chem **286**:20600–20605. http://dx.doi.org/10.1074/jbc.C110.204651.

21. **Morona R, Daniels C, Van Den Bosch L.** 2003. Genetic modulation of *Shigella flexneri* 2a lipopolysaccharide O antigen modal chain length reveals that it has been optimized for virulence. Microbiology **149**:925–939. http://dx.doi.org/10.1099/mic.0.26141-0.

22. **Morona R, Van Den Bosch L.** 2003. Lipopolysaccharide O antigen chains mask IcsA (VirG) in *Shigella flexneri*. FEMS Microbiol Lett **221**:173–180. http://dx.doi.org/10.1016/S0378-1097(03)00210-6.

23. **Daniels C, Morona R.** 1999. Analysis of *Shigella flexneri* Wzz (Rol) function by mutagenesis and cross-linking: *wzz* is able to oligomerize. Mol Microbiol **34**:181–194. http://dx.doi.org/10.1046/j.1365-2958.1999.01591.x.

24. **Bastin DA, Stevenson G, Brown PK, Haase A, Reeves PR.** 1993. Repeat unit polysaccharides of bacteria: a model for polymerization resembling that of ribosomes and fatty acid synthetase, with a novel mechanism for determining chain length. Mol Microbiol **7**:725–734. http://dx.doi.org/10.1111/j.1365-2958.1993.tb01163.x.

25. **Carter JA, Jimenez JC, Zaldivar M, Alvarez SA, Marolda CL, Valvano MA, Contreras I.** 2009. The cellular level of O-antigen polymerase Wzy determines chain length regulation by WzzB and Wzz$_{pHS-2}$ in *Shigella flexneri* 2a. Microbiology **155**:3260–3269. http://dx.doi.org/10.1099/mic.0.028944-0.

26. **Woodward R, Yi W, Li L, Zhao G, Eguchi H, Sridhar PR, Guo H, Song J K, Motari E, Cai L, Kelleher P, Liu X, Han W, Zhang W, Ding Y, Li M, Wang PG.** 2010. *In vitro* bacterial polysaccharide biosynthesis: defining the functions of Wzy and Wzz. Nat Chem Biol **6**:418–423. http://dx.doi.org/10.1038/nchembio.351.

27. **Tocilj A, Munger C, Proteau A, Morona R, Purins L, Ajamian E, Wagner J, Papadopoulos M, Van Den Bosch L, Rubinstein J L, Fethiere J, Matte A, Cygler M.** 2008. Bacterial polysaccharide co-polymerases share a common framework for control of polymer length. Nat Struct Mol Biol **15**:130–138. http://dx.doi.org/10.1038/nsmb.1374.

28. **Waldo GS, Standish BM, Berendzen J, Terwilliger TC.** 1999. Rapid protein-folding assay using green fluorescent protein. Nat Biotechnol **17**:691–695. http://dx.doi.org/10.1038/10904.

29. **Drew D, Lerch M, Kunji E, Slotboom DJ, de Gier JW.** 2006. Optimization of membrane protein overexpression and purification using GFP fusions. Nat Methods **3**:303–313. http://dx.doi.org/10.1038/nmeth0406-303.

30. **Murray GL, Attridge SR, Morona R.** 2003. Regulation of *Salmonella typhimurium* lipopolysaccharide O antigen chain length is required for virulence; identification of FepE as a second Wzz. Mol Microbiol **47**:1395–1406. http://dx.doi.org/10.1046/j.1365-2958.2003.03383.x.

31. **Tsai CM, Frasch CE.** 1982. A sensitive silver stain for detecting lipopolysaccharides in polyacrylamide gels. Anal Biochem **119**:115–119. http://dx.doi.org/10.1016/0003-2697(82)90673-X.

32. **Purins L, Van Den Bosch L, Richardson V, Morona R.** 2008. Coiled-coil regions play a role in the function of the *Shigella flexneri* O-antigen chain length regulator Wzz$_{pHS-2}$. Microbiology **154**:1104–1116. http://dx.doi.org/10.1099/mic.0.2007/014225-0.

33. **Mavris M, Manning PA, Morona R.** 1997. Mechanism of bacteriophage SfII-mediated serotype conversion in *Shigella flexneri*. Mol Microbiol **26**:939–950. http://dx.doi.org/10.1046/j.1365-2958.1997.6301997.x.

34. **McKinney J, Guerrier-Takada C, Galan J, Altman S.** 2002. Tightly regulated gene expression system in *Salmonella enterica* serovar Typhimurium. J Bacteriol **184**:6056–6059. http://dx.doi.org/10.1128/JB.184.21.6056-6059.2002.

35. **Kim TH, Sebastian S, Pinkham J T, Ross RA, Blalock LT, Kasper DL.** 2010. Characterization of the O-antigen polymerase (Wzy) of *Francisella tularensis*. J Biol Chem **285**:27839–27849. http://dx.doi.org/10.1074/jbc.M110.143859.

36. **Knirel YA, Bystrova OV, Kocharova NA, Zahringer U, Pier GB.** 2006. Conserved and variable structural features in the lipopolysaccharide of *Pseudomonas aeruginosa*. J Endotoxin Res **12**:324–336. http://dx.doi.org/10.1179/096805106X118906.

37. **Reddy A, Cho J, Ling S, Reddy V, Shlykov M, Saier MH.** 2014. Reliability of nine programs of topological predictions and their application to integral membrane channel and carrier proteins. J Mol Microbiol Biotechnol **24**:161–190. http://dx.doi.org/10.1159/000363506.

38. **Kenyon JJ, Reeves PR.** 2013. The Wzy O-antigen polymerase of *Yersinia pseudotuberculosis* O:2a has a dependence on the Wzz chain-length determinant for efficient polymerization. FEMS Microbiol Lett **349**:163–170. http://dx.doi.org/10.1111/1574-6968.12311.

39. **Schwartz M.** 1976. The adsorption of coliphage lambda to its host: effect of variations in the surface density of receptor and in phage-receptor affinity. J Mol Biol **103**:521–536. http://dx.doi.org/10.1016/0022-2836(76)90215-1.

40. **Islam ST, Huszczynski SM, Nugent T, Gold AC, Lam JS.** 2013. Conserved-residue mutations in Wzy affect O-antigen polymerization and Wzz-mediated chain-length regulation in *Pseudomonas aeruginosa* PAO1. Sci Rep **3**:3441. http://dx.doi.org/10.1038/srep03441.

41. **Taylor VL, Udaskin ML, Islam ST, Lam JS.** 2013. The D3 bacteriophage alpha-polymerase inhibitor (Iap) peptide disrupts O-antigen biosynthesis through mimicry of the chain length regulator Wzz in *Pseudomonas aeruginosa*. J Bacteriol **195**:4735–4741. http://dx.doi.org/10.1128/JB.00903-13.